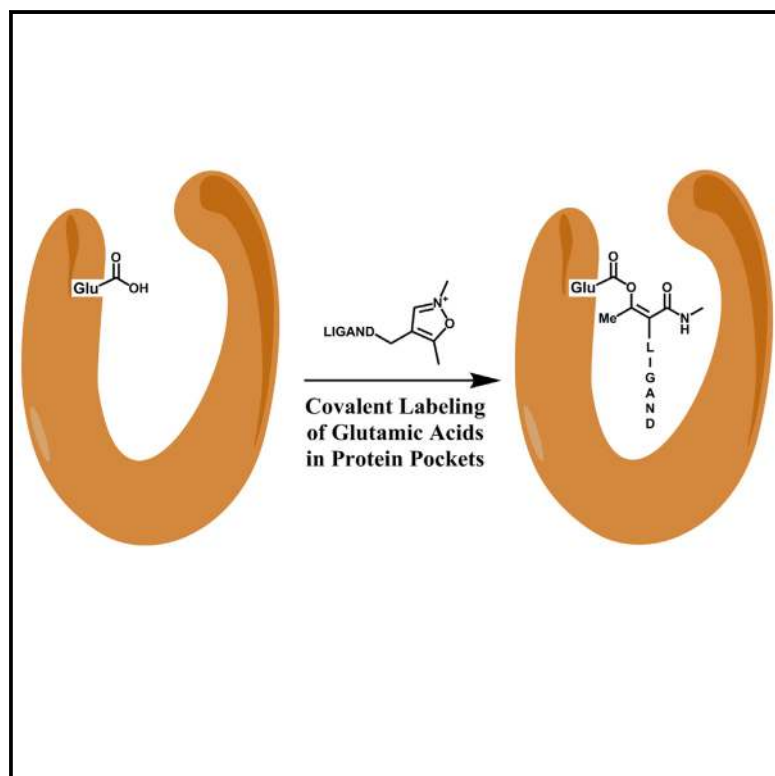


Cell Chemical Biology

Covalent Protein Labeling at Glutamic Acids

Graphical Abstract



Authors

Pablo Martín-Gago, Eyad K. Fansa, Michael Winzker, ..., Matthias Baumann, Alfred Wittinghofer, Herbert Waldmann

Correspondence

herbert.waldmann@mpi-dortmund.mpg.de

In Brief

Martín-Gago et al. have developed a novel class of covalent probes based on Woodward's reagent K that allows selective covalent labeling of glutamic acid residues inside protein binding pockets.

Highlights

- Chemical probes based on Woodward's reagent K (WRK) are reactive, covalent inhibitors
- WRK-derived probes selectively target glutamic acids in binding pockets
- Covalent binding occurs with high selectivity in cell lysate
- Inhibition of PDE6 δ with WRK-derived probes overcomes Arl2-mediated inhibitor release

Data Resources

5NAL



Covalent Protein Labeling at Glutamic Acids

Pablo Martín-Gago,¹ Eyad K. Fansa,² Michael Winzker,¹ Sandip Murarka,¹ Petra Janning,¹ Carsten Schultz-Fademrecht,⁴ Matthias Baumann,⁴ Alfred Wittinghofer,² and Herbert Waldmann^{1,3,5,*}

¹Department of Chemical Biology, Max Planck Institute of Molecular Physiology, Otto-Hahn Straße 11

²Structural Biology Group, Max Planck Institute of Molecular Physiology

³Faculty of Chemistry and Chemical Biology, Technische Universität Dortmund, Otto-Hahn Straße 6

⁴Lead Discovery Center GmbH

44227 Dortmund, Germany

⁵Lead Contact

*Correspondence: herbert.waldmann@mpi-dortmund.mpg.de

<http://dx.doi.org/10.1016/j.chembiol.2017.03.015>

SUMMARY

Covalent labeling of amino acids in proteins by reactive small molecules, in particular at cysteine SH and lysine NH groups, is a powerful approach to identify and characterize proteins and their functions. However, for the less-reactive carboxylic acids present in Asp and Glu, hardly any methodology is available. Employing the lipoprotein binding chaperone PDE6 δ as an example, we demonstrate that incorporation of isoxazolium salts that resemble the structure and reactivity of Woodward's reagent K into protein ligands provides a novel method for selective covalent targeting of binding site carboxylic acids in whole proteomes. Covalent adduct formation occurs via rapid formation of enol esters and the covalent bond is stable even in the presence of strong nucleophiles. This new method promises to open up hitherto unexplored opportunities for chemical biology research.

INTRODUCTION

Covalent protein targeting, in particular as explored in activity-based proteome profiling (ABPP) is a powerful method to identify and investigate the biological function of proteins (Speers and Cravatt, 2004). Typically in this approach, selective probes with balanced and often with attenuated electrophilic reactivity are employed to target protein nucleophiles in enzymes (Gersch et al., 2012; Niphakis and Cravatt, 2014; Shannon and Weerapana, 2015) and other proteins (Backus et al., 2016; Liu et al., 2013; Serafimova et al., 2012; Takaoka et al., 2013). A variety of different electrophiles and scaffolds has successfully been employed for covalent protein targeting. In the overwhelming majority of the cases nucleophilic cysteines and lysines (Akçay et al., 2016; Baillie, 2016; Fujishima et al., 2012; Gersch et al., 2012; Kato et al., 2005; Matsuo et al., 2013; Niphakis and Cravatt, 2014; Shannon and Weerapana, 2015; Takaoka et al., 2013, 2015; Tsuboi et al., 2011) are covalently labeled, although also other less-reactive amino acids, in particular serine, tyrosine, and histidine, are also amenable to modification (Dekker

et al., 2010; Fujishima et al., 2012; Liu et al., 1999; Matsuo et al., 2013; Tamura et al., 2012; Tsai et al., 2013).

Given the significance and widespread application and use of this approach, its extension to other amino acids is of major importance, in particular if their intrinsic nucleophilicity is low, such as the carboxylic acid groups in aspartic and glutamic acid. The corresponding probes must be of higher but still balanced reactivity to avoid unspecific protein labeling and deactivation of the electrophile by other cellular nucleophiles. Covalent labeling of Glu and Asp residues has been observed only in isolated cases, employing tosylates, fluorosugars, photo-activatable tetrazoles, or diazo compounds as reactive groups and mainly targeting exposed residues (Li et al., 2016; Mix and Raines, 2015; Tsukiji and Hamachi, 2014; Vocadlo and Bertozzi, 2004; Zhao et al., 2016). Therefore, the development of novel strategies for selective covalent modification of these carboxylic acids in the binding sites of proteins is highly desirable.

Woodward's reagent K (WRK) (Kemp and Chien, 1967; Woodward et al., 1961) (Figure 1A) has been employed in protein chemistry to covalently modify nucleophilic cysteine (Bustos et al., 1996), histidine (Carvajal et al., 2004), and carboxylic acid residues (Bodlaender et al., 1969; Feinstein et al., 1969; Komissarov et al., 1995; Mahnam et al., 2008; Pétra and Neurath, 1971; Pétra, 1971; Sinha and Brewer, 1985) in order to study enzymatic activity. We have recently described that ABPP probes based on WRK can be surprisingly selective and covalently modify the N-terminal proline of macrophage migration inhibitory factor (Qian et al., 2016).

Here we report that incorporation of WRK-based electrophiles into protein ligand scaffolds enables selective targeting of carboxylic acids in protein binding sites.

RESULTS

Design of Covalent WRK Probes for PDE6 δ

To establish the method, we focused on the lipoprotein chaperone PDE6 δ that binds prenylated GTPases such as Ras and Rheb (Papke et al., 2016; Zimmermann et al., 2013). bis-Sulfonamides, e.g., **6** (Figure 1B), bind to the PDE6 δ prenyl-binding site with sub-nanomolar affinity (Martín-Gago et al., 2017), but binding is antagonized by an allosteric interaction of PDE6 δ with the Arl2/3 GTPases, which results in release of medium- and even high-affinity cargo (Ismail et al., 2011; Martín-Gago et al., 2017).

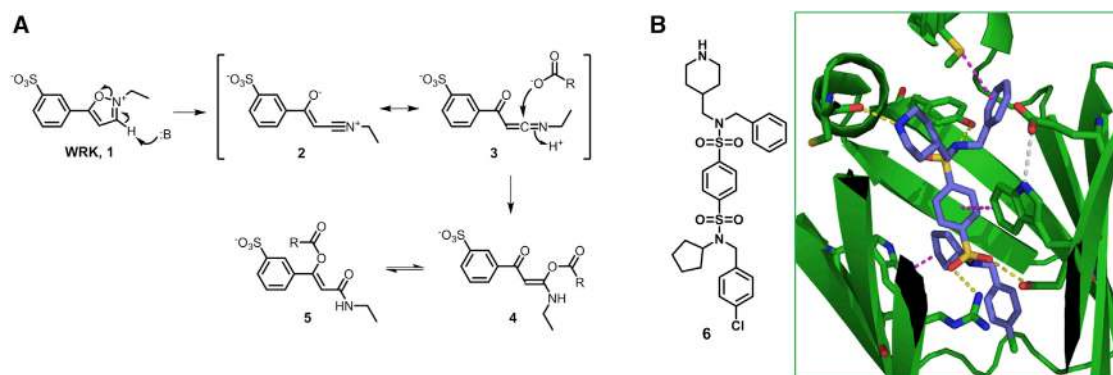


Figure 1. Rearrangement of Woodward's Reagent K into a Reactive Electrophile and Structural Basis for Equipment of PDE6 δ Ligands with a WRK-Derived Oxazolium Salt

(A) Base-induced rearrangement of WRK.

(B) Chemical and crystal structure of inhibitor **6** (PDB: 5ML8) in complex with PDE6 δ . Important H-bonding interactions of the ligand to the protein (dotted yellow line), between PDE6 δ residues (gray) and aromatic- π interactions (blue) are shown.

Covalent modification of an amino acid in the PDE6 δ binding site should abrogate inhibitor release. However, the prenyl-binding pocket does not display cysteine or lysine residues available for targeting (Murarka et al., 2016; Zimmermann et al., 2014). Instead, we reasoned that glutamic acid 88 (Glu88), at the upper end of the binding site close to the exit, would be a suitable site for covalent modification by a matching reactive group in the ligand.

Initially, a bis-sulfonamide was equipped with different tosylates (see the Supplemental Information; Figure S1), since this functional group can label glutamic acids in proteins (Tsukiji and Hamachi, 2014; Tsukiji et al., 2009). Indeed, covalent attachment of a corresponding ligand to PDE6 δ was observed by mass spectrometry. However, despite variation of electrophilic reactivity and linker length, labeling efficiency was low and reached 40% at the most.

Isloxazolium salts such as WRK undergo base-mediated ring opening to form ketenimines such as **3** (Figure 1A). These electrophiles react with carboxylic acids to enamides **4**, which can rearrange to more stable enol esters **5** (Woodward and Olofson, 1961; Woodward et al., 1961) and can be isolated (Bodlaender et al., 1969; Komissarov et al., 1995; Llamas et al., 1986).

Molecular-docking calculations (Schrödinger, Maestro suite, see Figures S4A and S4B) suggested that replacement of the phenyl ring in guiding inhibitor **6** with an N-methylisoxazolium ring linked by two (**12**) or four (**13**) methylene units (Figure 2A; for syntheses of the inhibitors, see the Supplemental Information) should enable covalent binding to Glu88, and both compounds formed the desired bond in less than 30 min. PDE6 δ was slowly reactivated within 24 hr (Figures S3A, S2C, and S2E). Adduct stability could be enhanced by introduction of a 5-methyl substituent (compounds **14** and **15**, Figure 2A). The fully substituted enol ester remained stable (Figures S2G and S2I) and labeling efficiency increased to $\geq 95\%$. Incorporation of a piperidin-4-ylmethyl H bond donor, to form an additional H bond with the carbonyl group of C56 (compound **16**, Figures 2A and 2B) and variation of linker length (**12** versus **13** and **14** versus **15**) did not change the efficiency of the label-

ing, which proceeds in less than 10 min (Figure S2J). However, removal of the non-reactive sulfonamide substituents (compound **17**, Figure 2A) abrogates adduct formation, which indicates that correct orientation and proximity of the isoxazolium salt to the possible target Glu88 are necessary for covalent bond formation. As expected, the isoxazole precursors of compounds **12–16** (Figure S3D, **18–24**) did not covalently bind to PDE6 δ .

The chemical stability of representative isoxazolium salt **15** at 37°C proved to be high, moderate, and low at pH 1, 7.4, and 9, respectively (see Figure S6G). We also considered the reactivity of compound **15** to simple amino acids with side chains incorporating an acid, a thiol, an amide, and an alcohol (i.e., Glu/Asp, Cys, Lys, and Ser) at different concentrations and time points (Figure S7J). We observed 15% and 20% enol ester formation in the presence of 30 μM Glu or Asp after 30 and 60 min reaction, respectively. The conjugation product was not detected at lower concentrations. When using Cys, we found 34% and 50% adduct formation at the same time points. The reactivity of isoxazolium salts with thiols has been described previously (Llamas et al., 1986). We did not find adduct formation when using Ser or Lys as nucleophiles.

Identification of the Labeling Site

To identify the labeling site, binding to PDE6 δ E88A mutant (PDE6 δ^{E88A}) was analyzed in a fluorescence polarization assay using a known fluorescently labeled PDE6 δ inhibitor (**25-L***, Figure S3) (Papke et al., 2016; Zimmermann et al., 2013). The PDE6 δ^{E88A} mutant showed similar binding affinity ($K_D = 5.9 \pm 2.1$ nM) toward **25-L*** than PDE6 δ^{WT} ($K_D = 2.6 \pm 1.3$ nM) (Figure S3E). This indicates that the mutant is properly folded and interacts with PDE6 δ inhibitors in a comparable mode as the wild-type protein. Compounds **14–16** did not bind to the E88A mutant (Figure 3), even at a 30-fold excess. Notably, under these conditions, the mutant was not labeled although it contains a variety of additional reactive residues including Cys, Lys, His, Glu, and Asp (Figures 3 and S5A–S5C). In addition, **16** did not bind covalently to further proteins, i.e., Arl2, HRas^{G12D}, GST, or BSA (Figures S5D–S5I).

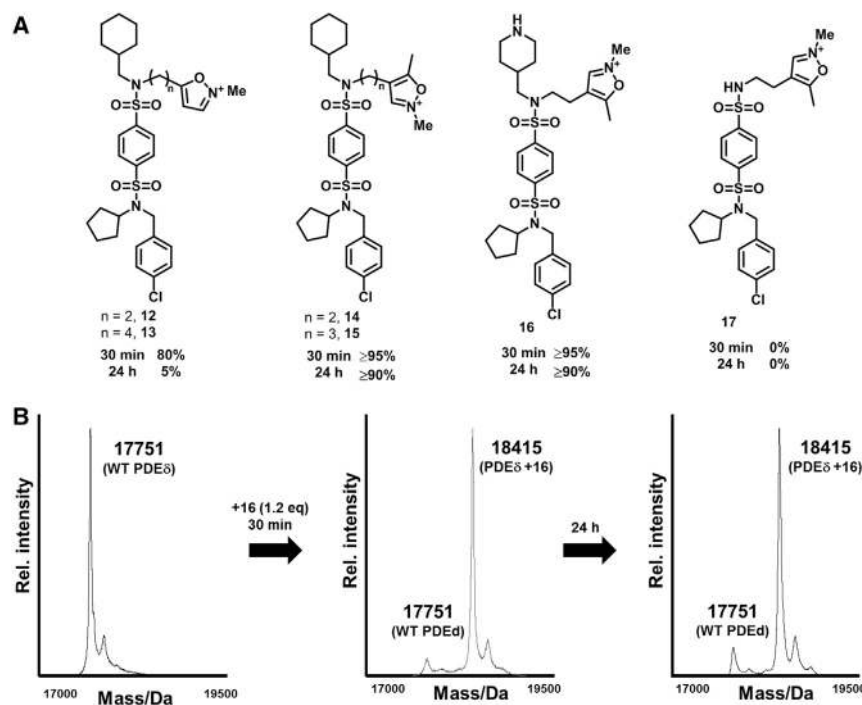


Figure 2. Chemical Structures of Compounds 12–17 and Tethering Assay for Compound 16

(A) Chemical structures of inhibitors **12–17** bearing a WRK-inspired warhead. Percentages represent adduct formation after 0.5 and 24 hr with 2.4 μM compound (1.2 eq) in HEPES buffer as determined by MALDI. Percentages of covalent adduct formation were estimated by area under the curve integration of the MALDI spectra.

(B) Positive ion mode MALDI-TOF mass spectra of WT-PDE6δ before, after 30 min, and after 24 hr incubation with compound **16** (2.4 μM, 1.2 eq). See also Figure S2.

icant after 90 and 300 min incubation, and does not change with excess Arl2. This demonstrates that even an excess of Arl2 does not allow binding of excess **T-26**, demonstrating that **15** remains covalently bound to PDE6δ.

Crystal Structure of a Covalent Inhibitor Bound to PDE6δ

The crystal structure of the adduct resulting from compound **15** in complex with

PDE6δ (Figure 6A) unambiguously proved covalent binding to Glu88 and revealed that the bis-sulfonamide part binds as observed for non-covalent inhibitors (Martín-Gago et al., 2017; see also Figure S4C). The electron density of the covalent link is slightly reduced in comparison with the rest of the ligand, which may reflect the presence of two different covalent adducts due to intramolecular acyl transfer (see Figure 1).

The covalent adduct is chemically fairly stable, since treatment of adducts formed between compounds **14–16** and PDE6δ with a 50-fold excess of NH₂OH (Bodlaender et al., 1969; Feinstein et al., 1969; Komissarov et al., 1995) did not result in ligand release even in the presence of the release factor Arl2 (Figure S7).

Selective PDE6δ Engagement in Cell Lysate

To prove physical PDE6δ engagement by inhibitor **16** in a cellular environment, we performed a cellular thermal shift assay (CETSA) using mass spectrometric readout (Franken et al., 2015; Reinhard et al., 2015; Savitski et al., 2014). Proteins were considered hits when they showed a characteristic shift in melting temperature higher than 2°C upon ligand binding, or when a stabilization in the recorded signal intensities at the highest two temperatures was at least 5% (see the Supplemental Information for details). The CETSA experiment (Figure 6B) revealed that ligand **16** only engaged PDE6δ, GDPGP1, PSMG3, and PTGES2. Considering the high prevalence of carboxylic acid groups in proteins, this covalent inhibitor targets PDE6δ with a high degree of selectivity.

Comparison of thermal stabilization by compound **16** with the corresponding non-reactive precursor **23** ($K_D = 53 \pm 9$ nM, Figure S3D) and derivative **24** ($K_D = 98 \pm 21$ nM, Figure S3D), which contains a deactivated hydrolyzed warhead, revealed that stabilization by covalent ligand **16** was markedly higher than observed for non-covalent medium-affinity ligands **23** and **24** (Figure 6C).

Covalently Bound Inhibitors Cannot Be Released by Arl2

The small GTP binding protein Arl2 binds to an allosteric site of PDE6δ, and thereby induces release of cargo from the prenyl-binding pocket (Ismail et al., 2011). Covalent binding of compounds **14–16** to Glu88 of PDE6δ is not prevented by Arl2, as shown by addition of the inhibitors to a preformed Arl2/PDE6δ complex (Figure S6).

As expected, Arl2 cannot release covalently bound ligands from the PDE6δ binding pocket. Addition of an excess of competitor **25** (Figure S3C) and subsequent addition of Arl2 to preformed adducts between PDE6δ and compounds **14–16** shows that the peak in the MALDI for the covalent product remains and that the covalent linkage is not disrupted (Figure 4). To further corroborate this finding, we established an Arl2 release experiment based on a fluorescence-quenching assay using fluorescein/carboxytetramethylrhodamine (TAMRA) as fluorophore/quencher pair (Figure 5A). Addition of a high-affinity TAMRA-labeled PDE6δ ligand described earlier (**T-26**, $K_D = 5.3 \pm 1.5$ nM; Zimmermann et al., 2013; Figure S3C) to fluorescein-labeled PDE6δ (F-PDE6δ) results in fluorescence quenching (Figure 5B). Subsequent addition of Arl2 does not release the compound. Addition of an excess of **T-26** to a preformed complex of F-PDE6δ with the non-labeled sub-nanomolar inhibitor **25** ($K_D = 358 \pm 36$ pM; Martín-Gago et al., 2017; Figure S3C) does not lead to quenching, since **T-26** cannot readily compete **25** due to the higher affinity of the latter compound (Figure 5C). In the presence of the release factor Arl2 there is a slow exchange of **25** by **T-26**, as indicated by increasing quenching of F-PDE6δ fluorescence. When inhibitor **25** is replaced by the covalent inhibitor **15** under the same conditions, there is, depending on the incubation times before addition of **T-26**, very little quenching (Figures 5D–5F). Immediately after addition of **T-26**, there is a small drop in fluorescence (Figure 5D) which becomes insignif-

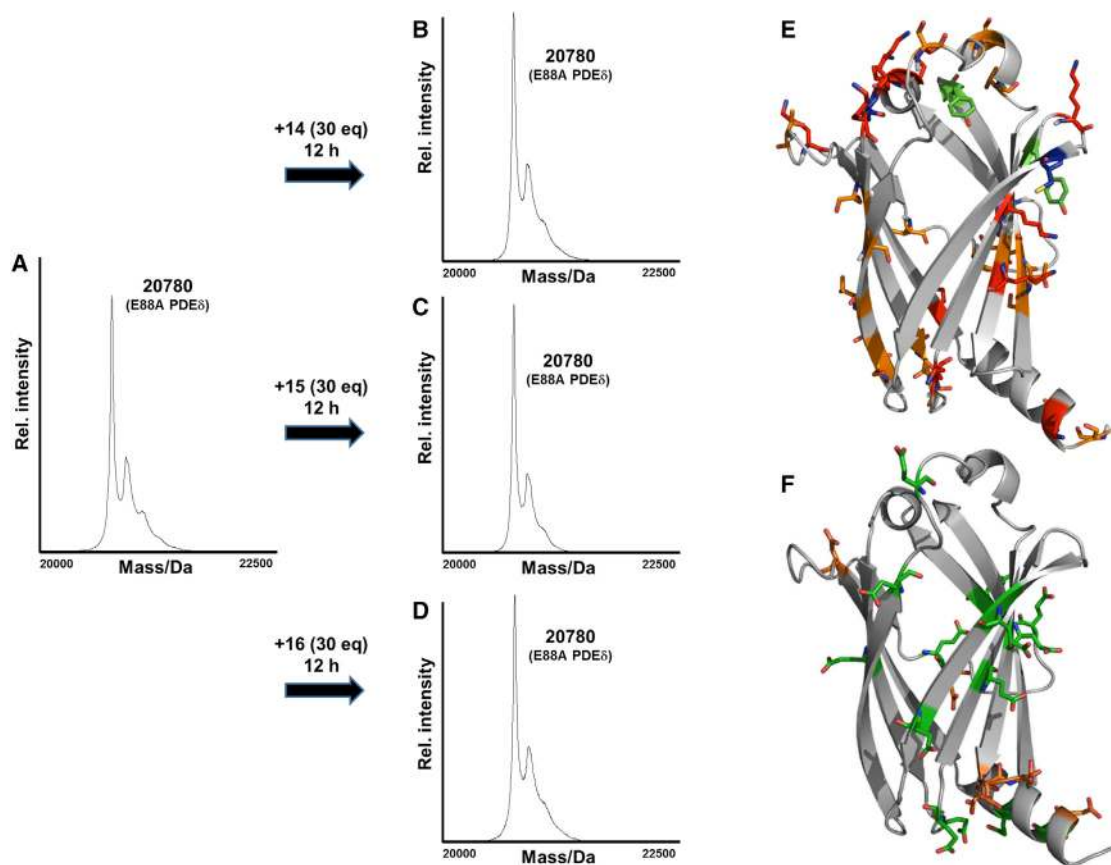


Figure 3. Identification of the Binding Site in the PDE6^δ Prenyl-Binding Pocket

(A–D) Left: positive ion mode MALDI-TOF mass spectra of His-tagged PDE6^δ^{E88A} before (A) and after (B–D) 12 hr incubation with compounds **14**, **15**, and **16** (30 eq), respectively. Right: stick representation of nucleophilic residues in PDE6^δ^{E88A}.

(E) Cys (C56, C86; blue), Thr (T27, T35, T68, T102, T104, T124, T131, T142; orange), Ser (S02, S39, S60, S66, S67, S101, S107, S115, S121, S141; orange), Tyr (Y81, Y149; green), Lys (K04, K16, K29, K51, K52, K55, K57, K73, K79, K83, K132; red), and His (H45; magenta).

(F) Glu (E6, E10, E36, E44, E46, E62, E69, E72, E77, E89, E93, E110, E114, E130; green) and Asp (D18, D21, D64, D100, D103, D126; orange).

DISCUSSION AND CONCLUSION

The development and application of small-molecule probes that covalently label target proteins based on enzyme mechanism (ABPP) (Jessani and Cravatt, 2004) or proximity of functional groups with complementary reactivity (Takaoka et al., 2013) is a powerful method for the study of protein function. This approach is best established for covalent modification of amino acids with fairly reactive nucleophilic side chains, i.e., cysteine and lysine, by means of electrophilic reagents with attenuated reactivity.

The development of a reagent class that would enable the covalent labeling of the less-nucleophilic glutamic and aspartic acids would significantly broaden the applicability of the approach in general. Importantly, Glu and Asp occur in binding sites (4.9% and 5.7%, respectively) with similar frequency than Lys (5.1%), but three times more often than Cys residues (1.5%) (Chen and Kurgan, 2009). While in individual cases carboxylic acids have been targeted covalently (Tamura et al., 2012; Vocadlo and Bertozzi, 2004; Weerapana et al., 2008), novel methods are in high demand.

Functional groups that enable covalent labeling of Glu and Asp in general need to have higher reactivity than established

electrophiles. However, reactivity must be balanced to avoid unspecific side reactions and labeling or deactivation in lysate. Therefore, their reactivity should be tunable by introduction of appropriate substituents. In addition, the covalent adducts formed should be sufficiently stable to enable analysis of protein function. We reasoned that isoxazolium salts represented by WRK might meet these demands. WRK was originally used as a carboxylic acid-activating reagent in peptide synthesis. As such it is stable, but it can be activated by bases initiating a rearrangement to form a ketenimine that reacts with carboxylic acids to form enol esters. Due to this reactivity, WRK has also been employed in enzymology for analysis of enzyme mechanisms through covalent modification of key carboxylic acids and other amino acids (Bustos et al., 1996; Carvajal et al., 2004; Komissarov et al., 1995; Mahnam et al., 2008; Sinha and Brewer, 1985).

We envisaged that incorporation of a WRK-derived functional group into protein ligands could open up a general opportunity to covalently modify Glu and Asp in protein binding sites. The base-mediated rearrangement could be initiated by appropriate functional groups in the protein, and the ketenimine formed would then react with a carboxylic acid in close proximity. The resulting

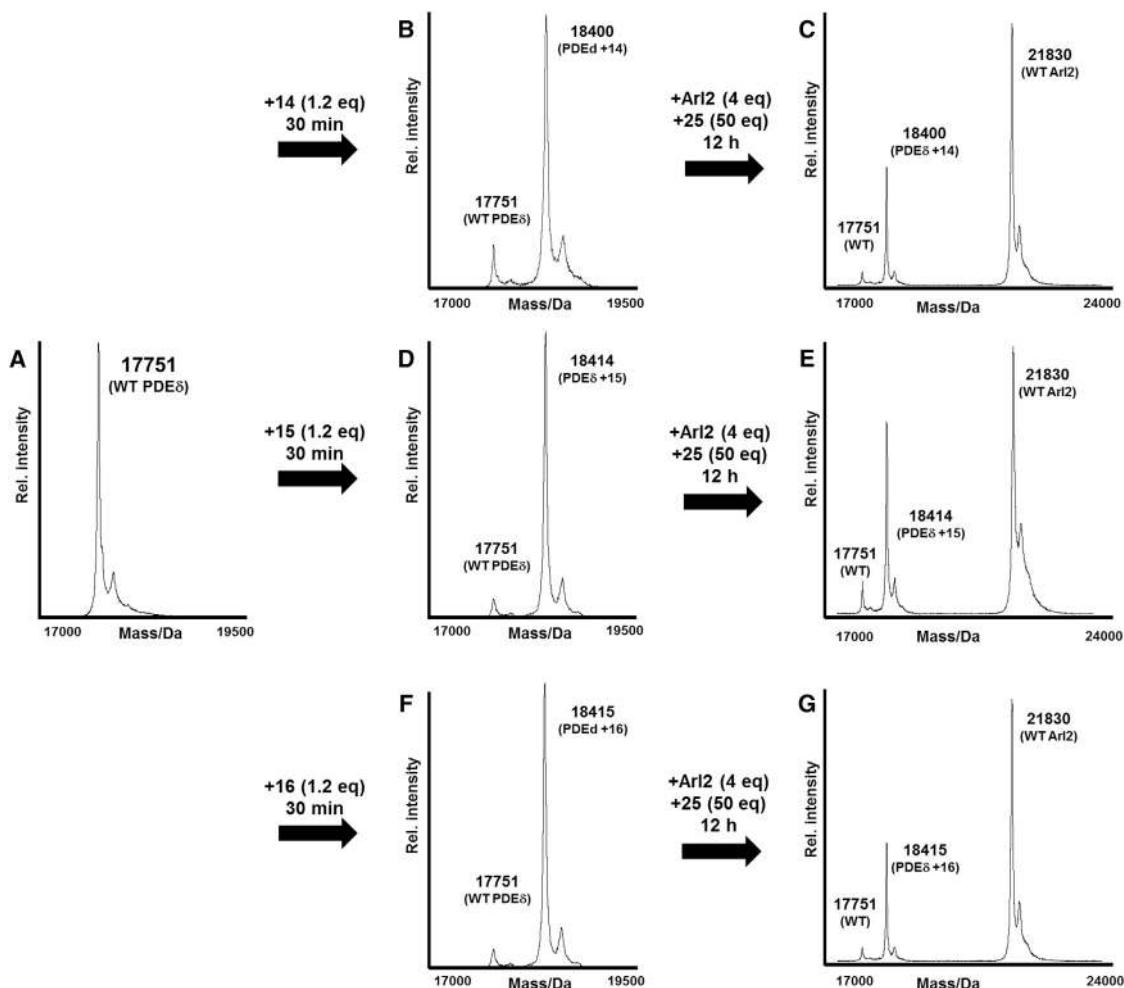


Figure 4. Mass Spectrometric Determination that Covalently Bound Inhibitors Cannot Be Released by Arl2

Positive ion mode MALDI-TOF mass spectra of PDE6 δ (A) and covalently bound to **14** (B), **15** (D), and **16** (F) before and after addition of His-tagged Arl2 and unlabeled competitor **25** (C, E, and G).

enol ester would be fairly stable because subsequent nucleophilic attack and hydrolytic reversal of the covalent tagging might be prevented by the binding site itself, thereby guaranteeing longer lifetime of the covalent adduct. In addition, the reactivity of the covalent probes, by analogy to the reactivity of isoxazolium salts in general (Woodward et al., 1961), would be adjustable by introduction of appropriate substituents.

As a representative example to provide proof-of-principle we chose PDE6 δ , a prenyl protein binding chaperone that binds the prenylated C termini of GTPases such as Ras and Rheb (Chandra et al., 2012). We have previously developed high-affinity inhibitors of these interactions that bind to the prenyl-binding site of the chaperone (Martín-Gago et al., 2017; Papke et al., 2016; Zimmermann et al., 2013). However, inhibitor binding is antagonized by the Arl2/3 proteins that stabilize PDE6 δ in the so-called closed conformation and thereby induce ligand release. In the binding site, nucleophilic amino acids, in particular cysteine and lysine, are not available that could be targeted for covalent modification to overcome Arl2/3-mediated release. However, the prenyl-binding site embodies a glutamic acid

(Glu88) close to the exit of the prenyl-binding tunnel. Thus, equipment of a high-affinity inhibitor of the PDE6 δ -cargo interaction with an isoxazolium group resembling the structure of WRK would be an equally interesting, novel, and relevant case to establish the methodology.

Based on molecular modeling considerations, a phenyl group in the inhibitor that is in close proximity to Glu88 was replaced by isoxazolium groups. After structure optimization by introduction of an additional, stabilizing substituent, a covalent PDE6 δ inhibitor was identified that is indeed activated in the binding site and rapidly forms a covalent bond to Glu88. The crystal structure of the corresponding inhibitor-protein complex proves the anticipated covalent binding mode and indicates that two isomeric enol esters may have been formed, which can, in principle, be interconverted by an acyl shift. The covalent adduct is stable to treatment with excess of a potent nucleophile. Target engagement occurs in the cell lysate with high selectivity, as proven by means of a cellular thermal shift experiment.

These findings provide proof-of-principle for the notion that fairly reactive functional groups can be engineered and

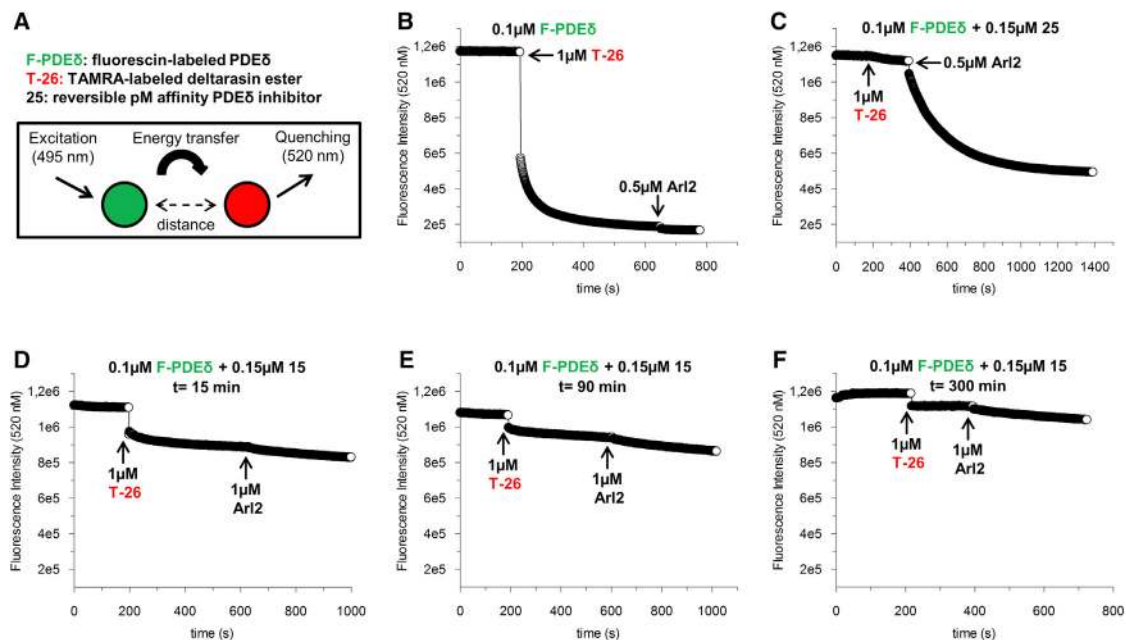


Figure 5. Determination that Covalently Bound Inhibitors Cannot Be Released by Arl2 Employing a Fluorescence-Quenching Assay

(A) Schematic representation of the quenching assay.

(B) Binding of **T-26** to F-PDE6 δ results in quenching of fluorescence emission and the addition of Arl2 (620 s) cannot directly release the **T-26** from its complex with F-PDE6 δ .

(C) The presence of **25** in complex with PDE6 δ prevents the binding of **T-26**, which was added in high excess. The addition of a high excess of Arl2 (400 s) results in slow displacement of **25** by **T-26**, as indicated by the quenching of F-PDE6 δ .

(D–F) The presence of **15** in complex with PDE6 δ (with different incubation times) prevents the binding of **T-26**. The addition of an excess of Arl2 does not lead to the displacement of **15** by an excess of **T-26**, as indicated by the stable emission intensity of F-PDE6 δ . The chemical structures and affinity K_D values for PDE6 δ of the compounds can be found in the [Supplemental Information \(Figure S3C\)](#).

employed for the successful development of covalent inhibitors targeting carboxylic acids with attenuated nucleophilic potency in protein pockets. For WRK-type isoxazolium salts this fine-tuning can be achieved by varying the steric demand and electronic properties of the heterocycle substituents (Woodman and Davidson, 1970; Woodward and Woodman, 1968; Woodward et al., 1961). However, reactivity may also translate into selectivity. Thus, solvent-exposed carboxylic acids may be converted into hydrolysis-sensitive enol esters, whereas analogous esters in binding sites will be protected from hydrolysis. Indeed, in the case detailed above, the core structure of the inhibitor guarantees rapid and tight binding of the inhibitor to the binding site (Martín-Gago et al., 2017), which then protects the covalent intermediate from nucleophilic attack. Such properties may be important, in general, for the successful application of probes containing reactive groups because competing unspecific protein binding and deactivation by nucleophiles present in cell lysate and cytosol will be suppressed. In addition, the moderate stability of isoxazolium salts in buffer at cellular pH provides this compound class with an inherent kinetic selectivity (Zaro et al., 2016). While tightly bound ligands will react rapidly with active site nucleophiles, excess unbound compound will eventually be hydrolyzed, thereby minimizing off-target labeling.

Future applications will need to explore the boundaries and balance of binding potency and chemical stability required for successful application of such covalent inhibitor classes. For WRK-type reactive ligands, we expect that equipment with sta-

bilizing substituents needs to be optimized on a case-to-case basis. Thus, tight and rapidly binding ligands (as the ones described here) may enable the use of more reactive isoxazolium salts than applicable in other ligand-protein binding events. Likewise, we expect that for application in whole-cell investigations, the stability of the WRK isoxazolium salts may have to be increased for compatibility with more extended incubation times and membrane permeability. Again, optimization may be necessary on a case-to-case basis.

The choice of PDE6 δ as an inaugurating example is of particular relevance. Previous inhibitor development for this protein was complicated by the fact that a cellular mechanism, independent of ligand binding to the target protein itself, counteracts inhibition, i.e., release of even high-affinity cargo from the PDE6 δ binding site by the Arl proteins (Martín-Gago et al., 2017). Our findings demonstrate that such limitations can be overcome by covalent inhibitors, even if they form a still reactive covalent adduct.

Since WRK initially was investigated as a carboxylic acid-activating reagent for peptide coupling (Woodward et al., 1961), by analogy it appears possible that also other peptide coupling reagent types (Al-Warhi et al., 2012), e.g., N-alkyl-2-halopyridinium salts (Mukaiyama, 1979), might serve as electrophilic groups in carboxylic acid-targeting covalent probes and reagents in a wider sense. Therefore, this approach in general may open up novel avenues of research in chemical proteomics in particular, and in chemical biology in general.

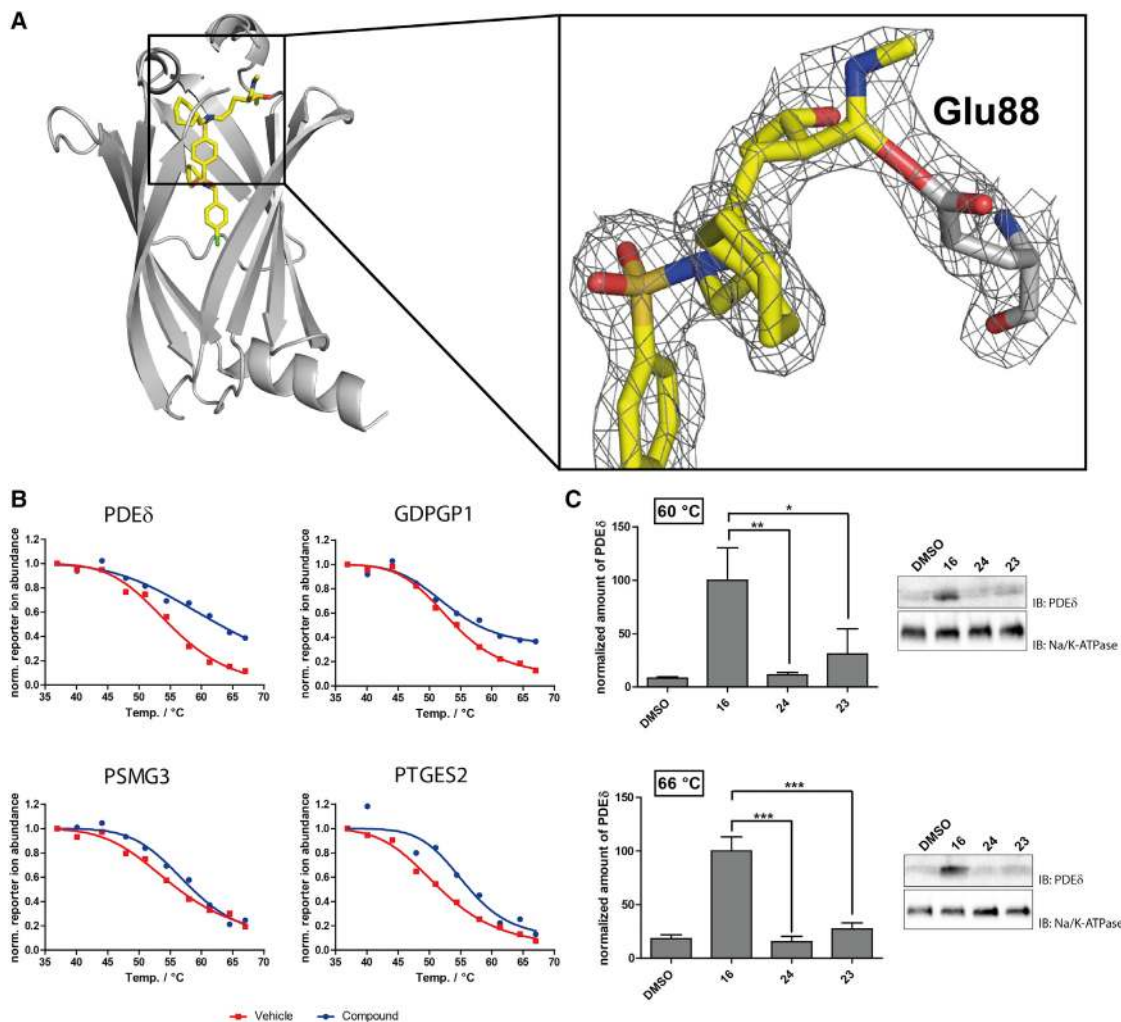


Figure 6. Crystal Structure of Inhibitor 15 in Complex with PDE6 δ and Target Engagement, CETSA

(A) Left: inhibitor **15** binds to PDE6 δ displaying the expected binding mode for this chemotype (see Figure S4C for a more detailed binding mode visualization). Right: $2F_o - F_c$ electron density map (1σ level) around the covalent bond between the carboxylic side-chain of Glu88 and the opened WRK warhead.

(B) Representative melting curves for PDE6 δ , GDPGP1, PSMG3, and PTGES2 as observed in a thermal protein profiling experiment. Melting curves for the DMSO controls are shown in red and melting curves after treatment with inhibitor **16** are shown in blue.

(C) Thermal stabilization of PDE6 δ in Jurkat lysate by the covalent inhibitor **16** is markedly higher than using the reversible ligand derivatives **23** and **24** at both 60°C and 66°C (1 μ M). Intensities of the PDE6 δ immunoblot bands (Image Lab) were plotted as mean \pm CI of 95% ($n = 4$). Statistical analysis was performed using one-way ANOVA test. * $p \leq 0.05$; ** $p \leq 0.01$; *** $p \leq 0.001$.

SIGNIFICANCE

The development of covalent inhibitors and probes that covalently bind to amino acids other than Cys and Lys residues is highly desirable. Using PDE6 δ as a model protein, the combination of an electrophilic warhead based on Woodward's reagent K and a potent inhibitor revealed that small molecules can be developed that bind selectively to the Glu88 residue inside the protein binding pocket. Even more demanding, covalent binding abrogates inhibitor release by the release factor Arl2 that removes even high-affinity cargo from PDE6 δ , thereby overcoming a severe limitation in the development of inhibitors for this protein. The compounds derived from the WRK electrophile rapidly

form stable covalent adducts, and labeling occurs in cell lysate with a high degree of selectivity. The high occurrence of Glu and Asp acids in binding sites suggests that WRK-derived isoxazolium salts may find widespread application in chemical proteomics and chemical biology in general.

STAR★METHODS

Detailed methods are provided in the online version of this paper and include the following:

- KEY RESOURCES TABLE
- CONTACT FOR REAGENT AND RESOURCE SHARING

● EXPERIMENTAL MODEL AND SUBJECT DETAILS

- Cell Lines

● METHODS DETAILS

- Protein Purification and Labeling
- Mass Spectrometric Determination of Covalent Labeling
- Crystallization and Structure Determination
- Fluorescence Quenching and Polarization Assays
- Molecular Modeling
- General Information for Cellular Thermal Shift Assay
- Cultivation and Harvesting of Cells, Cell Lysis
- Thermal Shift Assay
- Mass Spectrometry Based Readout of CETSA
- Melting Curves Calculation
- In-lysate Stabilization Assay
- Chemical Stability Assay
- Reaction of Compound 15 with Different Amino Acid Side-Chains
- Determination of K_D Values
- General Information for Chemical Synthesis

● QUANTIFICATION AND STATISTICAL ANALYSIS

● DATA AND SOFTWARE AVAILABILITY

- Data Resources

SUPPLEMENTAL INFORMATION

Supplemental Information includes seven figures, one table, and supplemental text and can be found with this article online at <http://dx.doi.org/10.1016/j.chembiol.2017.03.015>.

AUTHOR CONTRIBUTIONS

P.M.-G. and H.W. designed the compounds. P.M.-G. synthesized the compounds and P.M.-G. and E.F. performed the biochemical and biophysical characterization experiments. M.W. and P.J. performed the CETSA experiments and M.W., P.J., and P.M.-G. analyzed the data. M.W. performed the in-lysate thermal stabilization assay. S.M. participated in the synthesis of the compounds. C.S.-F. and M.B. performed the stability assays. E.F. and A.W. solved the structure by X-ray crystallography and developed the fluorescence-quenching assay. P.M.-G. and H.W. conceived and designed the experiments. H.W. supervised the research project. P.M.-G. and H.W. wrote the manuscript supported by E.F. and A.W.

ACKNOWLEDGMENTS

This research was supported by the Deutsche Forschungsgemeinschaft (Sonderforschungsbereich SFB 642 to A.W. and H.W.), and the European Research Council under the European Union's Seventh Framework Program (FP7/2007–2013; ERC Grant 268309 to H.W. and ERC Grant 268782 to A.W.). We are grateful to Malte Metz and Andreas Brockmeyer for assistance in the cellular thermal shift assay.

Received: January 31, 2017

Revised: March 7, 2017

Accepted: March 24, 2017

Published: April 20, 2017

SUPPORTING CITATION

The following reference appears in the Supplemental Information: [Thuong et al., 2012](#).

REFERENCES

- Akçay, G., Belmonte, M.A., Aquila, B., Chuaqui, C., Hird, A.W., Lamb, M.L., Rawlins, P.B., Su, N., Tentarelli, S., Grimster, N.P., et al. (2016). Inhibition of Mcl-1 through covalent modification of a noncatalytic lysine side chain. *Nat. Chem. Biol.* **12**, 931–936.
- Al-Warhi, T.I., Al-Hazimi, H.M.A., and El-Faham, A. (2012). Recent development in peptide coupling reagents. *J. Saudi Chem. Soc.* **16**, 97–116.
- Backus, K.M., Correia, B.E., Lum, K.M., Forli, S., Horning, B.D., González-Pérez, G.E., Chatterjee, S., Lanning, B.R., Teijaro, J.R., Olson, A.J., et al. (2016). Proteome-wide covalent ligand discovery in native biological systems. *Nature* **534**, 570–574.
- Baillie, T.A. (2016). Targeted covalent inhibitors for drug design. *Angew. Chem. Int. Ed.* **55**, 13408–13421.
- Bodlaender, P., Feinstein, G., and Shaw, E. (1969). Use of isoxazolium salts for carboxyl group modification in proteins. Trypsin. *Biochem. J.* **8**, 4941–4949.
- Bustos, P., Gajardo, M.I., Gómez, C., Goldie, H., Cardemil, E., and Jabalquinto, A.M. (1996). Woodward's reagent K reacts with histidine and cysteine residues in *Escherichia coli* and *Saccharomyces cerevisiae* phosphoenolpyruvate carboxykinases. *J. Protein Chem.* **15**, 467–472.
- Carvajal, N., Uribe, E., López, V., and Salas, M. (2004). Inactivation of human liver arginase by Woodward's reagent K: evidence for reaction with His141. *Protein J.* **23**, 179–183.
- Chandra, A., Grecco, H.E., Pisupati, V., Perera, D., Cassidy, L., Skoulidis, F., Ismail, S.A., Hedberg, C., Hanzal-Bayer, M., Venkitaraman, A.R., et al. (2012). The GDI-like solubilizing factor PDE δ sustains the spatial organization and signalling of Ras family proteins. *Nat. Cell Biol.* **14**, 148–158.
- Chen, K., and Kurgan, L. (2009). Investigation of atomic level patterns in protein-small ligand interactions. *PLoS One* **4**, e4473.
- Cox, J., and Mann, M. (2008). MaxQuant enables high peptide identification rates, individualized p.p.b.-range mass accuracies and proteome-wide protein quantification. *Nat. Biotechnol.* **26**, 1367–1372.
- Dekker, F.J., Rocks, O., Vartak, N., Menninger, S., Hedberg, C., Balamurugan, R., Wetzel, S., Renner, S., Gerauer, M., Schölermann, B., et al. (2010). Small-molecule inhibition of APT1 affects Ras localization and signaling. *Nat. Chem. Biol.* **6**, 449–456.
- Emsley, P., Lohkamp, B., Scott, W.G., and Cowtan, K. (2010). Features and development of *Coot*. *Acta Crystallogr. Sect. D Biol. Crystallogr.* **66**, 486–501.
- Feinstein, G., Bodlaender, P., and Shaw, E. (1969). Modification of essential carboxylic acid side chains of trypsin. *Biochemistry* **8**, 4949–4955.
- Franken, H., Mathieson, T., Childs, D., Sweetman, G.M.A., Werner, T., Tögel, I., Doce, C., Gade, S., Bantscheff, M., Drewes, G., et al. (2015). Thermal proteome profiling for unbiased identification of direct and indirect drug targets using multiplexed quantitative mass spectrometry. *Nat. Protoc.* **10**, 1567–1593.
- Fujishima, S., Yasui, R., Miki, T., Ojida, A., and Hamachi, I. (2012). Ligand-directed acyl imidazole chemistry for labeling of membrane-bound proteins on live cells. *J. Am. Chem. Soc.* **134**, 3961–3964.
- Gersch, M., Kreuzer, J., Sieber, S.A., Böttcher, T., Sieber, S.A., Fenteany, G., Standaert, R.F., Lane, W.S., Choi, S., Corey, E.J., et al. (2012). Electrophilic natural products and their biological targets. *Nat. Prod. Rep.* **29**, 659.
- Ismail, S.A., Chen, Y.-X., Rusinova, A., Chandra, A., Bierbaum, M., Gremer, L., Triola, G., Waldmann, H., Bastiaens, P.I.H., and Wittinghofer, A. (2011). Arl2-GTP and Arl3-GTP regulate a GDI-like transport system for farnesylated cargo. *Nat. Chem. Biol.* **7**, 942–949.
- Jessani, N., and Cravatt, B.F. (2004). The development and application of methods for activity-based protein profiling. *Curr. Opin. Chem. Biol.* **8**, 54–59.
- Kato, D., Boatright, K.M., Berger, A.B., Nazif, T., Blum, G., Ryan, C., Chehade, K.A.H., Salvesen, G.S., and Bogoy, M. (2005). Activity-based probes that target diverse cysteine protease families. *Nat. Chem. Biol.* **1**, 33–38.
- Kemp, D.S., and Chien, S.W. (1967). A new peptide coupling reagent. *J. Am. Chem. Soc.* **89**, 2743–2745.
- Komissarov, A.A., Romanova, D.V., and Debabov, V.G. (1995). Complete inactivation of *Escherichia coli* uridine phosphorylase by modification of Asp5 with Woodward's reagent K. *J. Biol. Chem.* **270**, 10050–10055.

- Li, Z., Qian, L., Li, L., Bernhammer, J.C., Huynh, H.V., Lee, J.-S., and Yao, S.Q. (2016). Tetrazole photoclick chemistry: reinvestigating its suitability as a bio-orthogonal reaction and potential applications. *Angew. Chem. Int. Ed.* **55**, 2002–2006.
- Liu, Y., Patricelli, M.P., and Cravatt, B.F. (1999). Activity-based protein profiling: the serine hydrolases. *Proc. Natl. Acad. Sci. USA* **96**, 14694–14699.
- Liu, Q., Sabnis, Y., Zhao, Z., Zhang, T., Buhrlage, S.J., Jones, L.H., and Gray, N.S. (2013). Developing irreversible inhibitors of the protein kinase cysteinome. *Chem. Biol.* **20**, 146–159.
- Llamas, K., Owens, M., Blakeley, R.L., and Zerner, B. (1986). N-Ethyl-5-phenylisoxazolium 3'-sulfonate (Woodward's reagent K) as a reagent for nucleophilic side chains of proteins. *J. Am. Chem. Soc.* **108**, 5543–5548.
- Mahnam, K., Moosavi-Movahedi, A.A., Bahrami, H., Hossein Hakimelahi, G., Ataie, G., Jalili, S., Saboury, A.A., Ahmad, F., Safarian, S., Amanlou, M., et al. (2008). Efficient factors in protein modification: adenosine deaminase esterification by Woodward reagent K. *J. Iran. Chem. Soc.* **5**, 464–475.
- Martin-Gago, P., Fansa, E.K., Klein, C.H., Murarka, S., Janning, P., Schürmann, M., Metz, M., Ismail, S., Schultz-Fademrecht, C., Baumann, M., et al. (2017). A PDE6 δ -KRas inhibitor chemotype with up to seven H-bonds and picomolar affinity that prevents efficient inhibitor release by Arl2. *Angew. Chem. Int. Ed.* **56**, 2423–2428.
- Matsuo, K., Kioi, Y., Yasui, R., Takaoka, Y., Miki, T., Fujishima, S.-H., and Hamachi, I. (2013). One-step construction of caged carbonic anhydrase I using a ligand-directed acyl imidazole-based protein labeling method. *Chem. Sci.* **4**, 2573.
- Mix, K.A., and Raines, R.T. (2015). Optimized diazo scaffold for protein esterification. *Org. Lett.* **17**, 2358–2361.
- Mukaiyama, T. (1979). New synthetic reactions based on the onium salts of aza-arenes [new synthetic methods (29)]. *Angew. Chem. Int. Ed.* **18**, 707–721.
- Murarka, S., Martin-Gago, P., Schultz-Fademrecht, C., Al Saabi, A., Baumann, M., Fansa, E.K., Ismail, S., Nussbaumer, P., Wittinghofer, A., and Waldmann, H. (2016). Development of pyridazinone chemotypes targeting the PDE δ prenyl binding site. *Chemistry* <http://dx.doi.org/10.1002/chem.201603222>.
- Niphakis, M.J., and Cravatt, B.F. (2014). Enzyme inhibitor discovery by activity-based protein profiling. *Annu. Rev. Biochem.* **83**, 341–377.
- Papke, B., Murarka, S., Vogel, H.A., Martin-Gago, P., Kovacevic, M., Truxius, D.C., Fansa, E.K., Ismail, S., Zimmermann, G., Heinelt, K., et al. (2016). Identification of pyrazolopyridazinones as PDE δ inhibitors. *Nat. Commun.* **7**, 11360.
- Pétra, P.H. (1971). Modification of carboxyl groups in bovine carboxypeptidase A. I. Inactivation of the enzyme by N-ethyl-5-phenylisoxazolium-3'-sulfonate (Woodward's reagent K). *Biochemistry* **10**, 3163–3170.
- Pétra, P.H., and Neurath, H. (1971). Modification of carboxyl groups in bovine carboxypeptidase A. II. Chemical identification of a functional glutamic acid residue and other reactive groups. *Biochemistry* **10**, 3171–3177.
- Qian, Y., Schürmann, M., Janning, P., Hedberg, C., and Waldmann, H. (2016). Activity-based proteome profiling probes based on Woodward's reagent K with distinct target selectivity. *Angew. Chem. Int. Ed.* **55**, 7766–7771.
- Reinhard, F.B.M., Eberhard, D., Werner, T., Franken, H., Childs, D., Doce, C., Savitski, M.F., Huber, W., Bantscheff, M., Savitski, M.M., et al. (2015). Thermal proteome profiling monitors ligand interactions with cellular membrane proteins. *Nat. Methods* **12**, 1129–1131.
- Savitski, M.M., Reinhard, F.B.M., Franken, H., Werner, T., Savitski, M.F., Eberhard, D., Martinez Molina, D., Jafari, R., Dovega, R.B., Klaeger, S., et al. (2014). Tracking cancer drugs in living cells by thermal profiling of the proteome. *Science* **346**, 1255784.
- Serafimova, I.M., Pufall, M.A., Krishnan, S., Duda, K., Cohen, M.S., Maglathlin, R.L., McFarland, J.M., Miller, R.M., Frödin, M., and Taunton, J. (2012). Reversible targeting of noncatalytic cysteines with chemically tuned electrophiles. *Nat. Chem. Biol.* **8**, 471–476.
- Shannon, D.A., and Weerapana, E. (2015). Covalent protein modification: the current landscape of residue-specific electrophiles. *Curr. Opin. Chem. Biol.* **24**, 18–26.
- Sinha, U., and Brewer, J.M. (1985). A spectrophotometric method for quantitation of carboxyl group modification of proteins using Woodward's reagent K. *Anal. Biochem.* **151**, 327–333.
- Speers, A.E., and Cravatt, B.F. (2004). Chemical strategies for activity-based proteomics. *ChemBioChem* **5**, 41–47.
- Takaoka, Y., Ojida, A., and Hamachi, I. (2013). Protein organic chemistry and applications for labeling and engineering in live-cell systems. *Angew. Chem. Int. Ed.* **52**, 4088–4106.
- Takaoka, Y., Nishikawa, Y., Hashimoto, Y., Sasaki, K., and Hamachi, I. (2015). Ligand-directed dibromophenyl benzoate chemistry for rapid and selective acylation of intracellular natural proteins. *Chem. Sci.* **6**, 3217–3224.
- Tamura, T., Tsukiji, S., and Hamachi, I. (2012). Native FKBP12 engineering by ligand-directed tosyl chemistry: labeling properties and application to photo-cross-linking of protein complexes in vitro and in living cells. *J. Am. Chem. Soc.* **134**, 2216–2226.
- Thuong, M.B., Mann, A., and Wagner, A. (2012). Mild chemo-selective hydration of terminal alkynes catalysed by AgSbF₆. *Chem. Commun. (Camb.)* **48**, 434–436.
- Tsai, C.-S., Yen, H.-Y., Lin, M.-I., Tsai, T.-I., Wang, S.-Y., Huang, W.-I., Hsu, T.-L., Cheng, Y.-S.E., Fang, J.-M., and Wong, C.-H. (2013). Cell-permeable probe for identification and imaging of sialidases. *Proc. Natl. Acad. Sci. USA* **110**, 2466–2471.
- Tsuboi, K., Bachovchin, D.A., Speers, A.E., Spicer, T.P., Fernandez-Vega, V., Hodder, P., Rosen, H., and Cravatt, B.F. (2011). Potent and selective inhibitors of glutathione S-transferase omega 1 that impair cancer drug resistance. *J. Am. Chem. Soc.* **133**, 16605–16616.
- Tsukiji, S., and Hamachi, I. (2014). Ligand-directed tosyl chemistry for in situ native protein labeling and engineering in living systems: from basic properties to applications. *Curr. Opin. Chem. Biol.* **21**, 136–143.
- Tsukiji, S., Miyagawa, M., Takaoka, Y., Tamura, T., and Hamachi, I. (2009). Ligand-directed tosyl chemistry for protein labeling in vivo. *Nat. Chem. Biol.* **5**, 341–343.
- Vocadlo, D.J., and Bertozzi, C.R. (2004). A strategy for functional proteomic analysis of glycosidase activity from cell lysates. *Angew. Chem. Int. Ed.* **43**, 5338–5342.
- Weerapana, E., Simon, G.M., and Cravatt, B.F. (2008). Disparate proteome reactivity profiles of carbon electrophiles. *Nat. Chem. Biol.* **4**, 405–407.
- Winn, M.D., Ballard, C.C., Cowtan, K.D., Dodson, E.J., Emsley, P., Evans, P.R., Keegan, R.M., Krissinel, E.B., Leslie, A.G.W., McCoy, A., et al. (2011). Overview of the CCP4 suite and current developments. *Acta Crystallogr. D. Biol. Crystallogr.* **67**, 235–242.
- Woodman, D.J., and Davidson, A.I. (1970). N-tert-butyl-beta-acyloxycrotonamides. *J. Org. Chem.* **35**, 83–87.
- Woodward, R.B., and Olofson, R.A. (1961). The reaction of isoxazolium salts with bases. *J. Am. Chem. Soc.* **83**, 1007–1009.
- Woodward, R.B., and Woodman, D.J. (1968). Stable enol esters from N-tert-butyl-5-methylisoxazolium perchlorate. *J. Am. Chem. Soc.* **90**, 1371–1372.
- Woodward, R.B., Olofson, R.A., and Mayer, H. (1961). A new synthesis of peptides. *J. Am. Chem. Soc.* **83**, 1010–1012.
- Zaro, B.W., Whitby, L.R., Lum, K.M., and Cravatt, B.F. (2016). Metabolically labile fumarate esters impart kinetic selectivity to irreversible inhibitors. *J. Am. Chem. Soc.* **138**, 15841–15844.
- Zhao, S., Dai, J., Hu, M., Liu, C., Meng, R., Liu, X., Wang, C., and Luo, T. (2016). Photo-induced coupling reactions of tetrazoles with carboxylic acids in aqueous solution: application in protein labelling. *Chem. Commun.* **52**, 4702–4705.
- Zimmermann, G., Papke, B., Ismail, S., Vartak, N., Chandra, A., Hoffmann, M., Hahn, S.A., Triola, G., Wittinghofer, A., Bastiaens, P.I.H., et al. (2013). Small molecule inhibition of the KRAS-PDE δ interaction impairs oncogenic KRAS signalling. *Nature* **497**, 638–642.
- Zimmermann, G., Schultz-Fademrecht, C., Küchler, P., Murarka, S., Ismail, S., Triola, G., Nussbaumer, P., Wittinghofer, A., and Waldmann, H. (2014). Structure guided design and kinetic analysis of highly potent benzimidazole inhibitors targeting the PDE δ prenyl binding site. *J. Med. Chem.* **57**, 5435–5448.

STAR★METHODS

KEY RESOURCES TABLE

REAGENT or RESOURCE	SOURCE	IDENTIFIER
Antibodies		
Anti-PDE6D	Thermo Fisher Scientific	P5-22008; RRID: AB_11154288
Anti-Na/K-ATPase	abcam	ab76020; RRID: AB_1310695
Anti-mouse, HRP	Thermo Fisher Scientific	31430; RRID: AB_228307
Anti-rabbit, HRP	Thermo Fisher Scientific	31460; RRID: AB_228341
Bacterial and Virus Strains		
<i>Escherichia coli</i> strain BL21-CodonPlus(DE3)-RIL	Stratagene	230240
Chemicals, Peptides, and Recombinant Proteins		
Sinapic Acid	Sigma-Aldrich	D7927
DMSO	Sigma-Aldrich	D8418
RPMI 1640	PAN Biotech	P04-18047
Penicillin/Streptomycin	PAN Biotech	P06-07100
SuperSignal™ West Femto Maximum Sensitivity Substrate	Thermo Fisher Scientific	34095
TMT10plex	Thermo Fisher Scientific	90110
MEM NEAA (100x)	PAN Biotech	P08-32100
Fluorescein isothiocyanate isomer I	Sigma-Aldrich	F7250
See Chemistry Procedures for synthesis of additional compounds	This paper	N/A
Deposited Data		
Crystal structure of 15 covalently bound to PDE6D	This paper	PDB: 5NAL
Experimental Models: Cell Lines		
Jurkat, Clone E6-1	ATCC	TIB-152
Oligonucleotides		
Primer: PDE ^{6E88A} gggcaatgcctagcagaatggtcttcg	Sigma-Aldrich	N/A
Recombinant DNA		
pET28a	Novagen	69864-3
pET-20b	Novagen	69739-3
pGEX-4T-1	Amersham	27458001
Software and Algorithms		
XDS	MPI for Medical Research, Heidelberg	http://homes.mpimf-heidelberg.mpg.de/~kabsch/xds/
Coot	Emsley et al., 2010	https://www2.mrc-lmb.cam.ac.uk/personal/pemsley/coot/
CCP4	Winn et al., 2011	http://www.ccp4.ac.uk/
GraFit.5	Erithacus Software	http://www.erithacus.com/grafit/index.html
GraphPad Prism 5.03	GraphPad Software Inc.	http://www.graphpad.com/scientific-software/prism/
Image Lab (v5.2.1 build 11)	Bio-Rad Laboratories	N/A
MaxQuant software (v.1.5.3.30)	Cox and Mann, 2008	http://www.coxdocs.org/doku.php?id=maxquant:start
Maestro 10.5	Schrödinger	https://www.schrodinger.com/maestro
Solver Marco	This paper	N/A

CONTACT FOR REAGENT AND RESOURCE SHARING

Further information and requests for resources and reagents should be directed to the Lead Contact, Herbert Waldmann (herbert.waldmann@mpi-dortmund.mpg.de).

EXPERIMENTAL MODEL AND SUBJECT DETAILS

Cell Lines

Jurkat cells were maintained in RPMI 1640 Medium supplemented with 10% (v/v) fetal bovine serum (FBS), penicillin (100 U/mL), streptomycin (100 mg/mL) and 1x NEAA. All cell lines were grown at 37°C in a humidified 5% CO₂ atmosphere.

METHODS DETAILS

Protein Purification and Labeling

All proteins were expressed in *Escherichia coli* strain BL21-CodonPlus(DE3)-RIL. Cells were induced at OD ~0.6 with 100 μM IPTG and incubated at 20 °C overnight. Cells were harvested and lysed in lyses buffer (30 mM Tris-HCl, pH 7.5, 150 mM NaCl and 1 mM b-mercaptoethanol, 1 mM PMSF) using French press. Supernatant of C-terminal histidine-tagged full-length Arl2 (expressed from pET20b plasmid) was loaded onto a Ni-NTA column (QIAGEN). Protein was eluted with elution buffer (30 mM Tris-HCl, pH 7.5, 150 mM NaCl and 1 mM b-mercaptoethanol, 250 mM imidazole), followed by gel filtration on a Superdex 75 S26/60 column using elution buffer without imidazole. Supernatant of N-terminal GST-tagged PDE6δ (expressed from pGEX-4T-1 plasmid) was loaded onto a Glutathione Sepharose 4B column (GE healthcare). Protein was eluted with elution buffer (30 mM Tris-HCl, pH 7.5, 150 mM NaCl and 1 mM b-mercaptoethanol, 20 mM glutathione), followed by tag cleavage and gel filtration on a Superdex 75 S26/60 column using elution buffer without glutathione.

The PDE6δ^{E88A} mutant was generated by quick-change mutagenesis PCR using a single primer (gggcaatgcctagcagaatggtcttcg) and the N-terminal histidine-tagged protein (expressed from pET28a plasmid) was purified as described for Arl2. For PDE6δ labeling, 2 mg of protein was incubated with a 50-fold molar excess of Fluorescein isothiocyanate (FITC) in PBS buffer containing 1 mM TCEP for 1 hour at 4°C. The excess label was removed by a desalting column.

Mass Spectrometric Determination of Covalent Labeling

Proteins were incubated with the compounds in 20 mM HEPES, pH 7.5, 150 mM NaCl at room temperature. A saturated solution of sinapic acid (Aldrich) in H₂O (0.1% TFA) / ACN (2:1) was used as matrix. 1 μL of the samples was mixed with 10 μL of matrix, and 1 μL of this mixture was placed on an MTP 384 ground steel target plate and dried in air. Mass spectra were obtained over the *m/z* range 16.500–19.500 using a Bruker UltrafleXtreme TOF/TOF mass spectrometer. The *m/z* range was adjusted when other proteins were investigated (20.000–22.500 for His-tagged PDE6δ^{E88A}, 18.000–20.000 for HRas^{G12D}, 21.000–33.000 for GST, 61.000–73.000 for BSA and up to 23.000 for His-tagged Arl2).

Crystallization and Structure Determination

A stock solution of 50 mM **13** in DMSO was used for crystallization. A 1:1 molar ratio mixture of PDE6δ:**13** at final concentration of 500 μM was used for crystallization screening. Crystals appeared after 2 days and were flash frozen in a cryoprotectant solution that contains glycerol in addition to the mother liquor. Diffraction datasets were collected using in house facility. After data processing by XDS the structure was solved by Molrep from CCP4 (suite) using PDEδ from the PDEδ-farnesylated Rheb complex (PDB: 3T5G) as a search model for the molecular replacement. The model was built by WinCoot and refined by REFMAC5. Refinement and data collection statistics are summarized in [Table S1](#).

Fluorescence Quenching and Polarization Assays

Fluorescence measurements were carried out at 20 °C in buffer containing 25 mM Tris-HCl, pH 7.5, 150 mM NaCl and 3mM DTE, using Fluoromax-4 spectrophotometer (HORIBA JobinYvon, Munich, Germany). For the Fluorescence quenching assay fluorescein-labeled PDE6δ (F-PDE6δ) was excited at 490 nm and the quenching by TAMRA-labeled PDE6δ-inhibitor (T-Ester, **26**) was recorded by measuring the emission intensity at 520 nm. The fluorescence polarization measurements were carried out using fluorescein-labeled **25** with excitation and emission wavelengths at 495 nm and 520 nm. The data were analyzed with GraFit 5.0 program (Erithracus Software).

Molecular Modeling

Molecular modeling experiments were carried out with the Maestro 10.5 suite (Schrödinger). Both ligand and receptor flexibility were taken into account by using receptor docking (Glide) in combination with the protein structure prediction embedded in the program Prime. Protein Preparation Wizard (Schrödinger Maestro suite) was used to prepare the PDE6δ co-crystal for the calculations. Previously obtained X-ray structures were used to define the active site. Water molecules were removed from the protein crystal structure, hydrogen atoms were added and resulting structure was refined by OPLS2005 force-field. The minimization was ended when the RMSD reached 0.18 Å. Receptor Grid Preparation (Glide) was used to generate the protein grid that was subsequent utilized in

docking experiments. The Van der Waals radius scaling factor was set to 0.5 with a partial charge cutoff of 0.25. Arg61 was selected as a possible site for hydrogen bonding. Additionally, docking runs were carried out using additional hydrogen bond constraints with Tyr149, Cys56, Gln78 and/or Glu88. Ligand preparation for docking was carried out with LigPrep in Maestro 10.5 and the OPLS_2005 force-field. Epika was used to generate possible states at target pH 7.0 ± 4.0 . Ligand docking options in Glide were used for the first round of docking experiments. Under Setting, XP (extra precision), Dock flexibly, Sample nitrogen inversions, Sample ring conformation and Epik state penalties to docking score were selected, amide bonds were penalized for nonplanar conformation. Under the Ligands section, the Van der Waals radius scaling factor was set to 0.5 and the docking was set to match at least 1 out of two constraints. Several high-score binding poses were generated and co-crystallized compound **13** was re-docked and analyzed in terms of overlay with the X-ray structure.

General Information for Cellular Thermal Shift Assay

Three biological replicates employing lysates from Jurkat cells were measured in which compound **16** was used at a concentration of 1 μM and alternatively with DMSO (1 % v/v) treated samples as controls. The samples were split into 10 aliquots each and incubated at 10 different temperatures between 37 and 67 °C. The precipitated fraction of the proteins was centrifuged off and the soluble fraction quantified relatively to the lowest temperature using a 10plex TMT label mass spectrometry based approach, i.e. thermal protein profiling (TPP). Proteins were considered as stabilized or destabilized when, in all three replicates, 1) they had a shift in melting points of at least $\pm 2^\circ\text{C}$ (same direction) or 2) they showed a difference in the relative peak intensities of at least 5 % for the two highest temperatures. In total, we identified 5684 proteins, of which 3217 were identified with at least two unique peptides in all replicates (compound treated and DMSO controls). 2617 of these proteins showed a normal melting curve in the DMSO control, i.e. they had relative intensities of the labels of the two highest temperatures smaller or equal to 35 % of the labels of the lowest temperatures. Out of the 5684 proteins only PDE6 δ , GDPGP1, PSMG3 and PTGES2 were identified as hits according to the definition above. PDE6 δ showed a typical melting behavior only in the DMSO controls. In compound treated samples, the percentage of soluble protein at high temperatures ($T > 58^\circ\text{C}$) was much higher than in DMSO controls (see Figure 6B), i.e. the stabilization of PDE6 δ by **16** leads to an incomplete precipitation of the protein at higher temperatures.

Cultivation and Harvesting of Cells, Cell Lysis

Jurkat cells were cultivated until a cell density of $1.5\text{-}2.0 \times 10^6$ was reached. 50 ml of cell suspension were transferred into a falcon tube and incubated on ice for 2 min followed by centrifugation at 350 x g at room temperature for 3 min. The supernatant was discarded and the pellet re-suspended in 25 ml of ice-cold phosphate buffered saline (PBS). The cells were harvested by centrifugation at 350 x g at room temperature for 2 min and the supernatant discarded again. This washing procedure was repeated twice. After the last washing and centrifugation step, cells were re-suspended in 1.5 ml PBS and quickly frozen in liquid nitrogen. Cell lysis was performed via thaw/freezing cycles using liquid nitrogen. Therefore, frozen cells were thawed at 23°C until about 60-80 % of the cells were unfrozen and kept on ice until the whole sample was thawed. After that, cells were quickly frozen with liquid nitrogen again and the cycle was repeated 4 times. Afterwards, the cell lysate was centrifuged for 20 min at 100.000 x g at 4°C in an ultracentrifuge. The resulting supernatant was gently transferred into a new tube, quickly frozen with liquid nitrogen and stored at -80°C until further usage.

Thermal Shift Assay

Protein concentration was determined by using the Bradford method. Samples were diluted with PBS to a final protein concentration of around 4 mg/ml. Samples were divided into two aliquots. One of the aliquots was incubated with 14 μl of **16** solution (1 $\mu\text{mol/l}$ in DMSO) and the other aliquot was incubated with 14 μl of DMSO for 10 min at room temperature. Each of the aliquots was divided into 10 new aliquots with 100 μl each, which were incubated at the following temperatures for 3 min (1: 36.9°C, 2: 40.1°C, 3: 44.1°C, 4: 47.9°C, 5: 51.0°C, 6: 54.4°C, 7: 58°C, 8: 61.3°C, 9: 64.5°C, 10: 67°C). Afterwards, samples were allowed to cool for 5 min to room temperature and centrifuged for 20 min at 100.000 x g at 4°C in an ultracentrifuge.

Mass Spectrometry Based Readout of CETSA

For the mass spectrometry based readout samples were reduced, alkylated, precipitated with acetone and tryptic digested. After that, each aliquot was labeled using TMT reagents according to the temperature used during the thermal shift procedure. For reduction, to each 75 μl aliquot resulting from the thermal shift procedure 7.5 μl of 200mM TCEP (tris(2-carboxyethyl)phosphine) solution (prepared from 140 μl of 0.5 M TCEP, 140 μl H₂O and 70 μl 1M TEAB (triethylammonium bicarbonate buffer)) were added, mixed by inversion, shortly centrifuged at 10.000 x g and incubated at 55°C for 1 h in a thermo block. To alkylate, 7.5 μl of freshly prepared 375 mM iodoacetamide solution (26 mg iodoacetamide dissolved in 375 μl of 200 mM TEAB buffer) were added to each sample and incubated for 30 minutes in the dark at room temperature. For precipitation of proteins, six volumes of pre-chilled (-20°C) acetone were added and incubated at -20°C overnight. Afterwards, samples were centrifuged for 10 min at 8000 g at 4°C and the supernatants were disposed. The pellets were dried for about 30 to 45 min at room temperature and then re-suspended in 107.5 μl of trypsin solution (165 μl of a trypsin solution of 100 μg in 250 ml of 10 mM HCl diluted in 2200 μl of 100 mM TEAB buffer). Samples were vortexed for about 20 s and shortly centrifuged to gather the suspension at the bottom to the tube, followed by incubation at 37°C for 2-3 hours. Vortexing and centrifugation were repeated and samples were incubated at 37°C overnight. At the next day, samples were spun down and labeled with TMT label. Briefly, 82 μl of anhydrous acetonitrile were added to each 0.8 mg of TMT label

reagent aliquot (TMT10plex, #90110 ThermoFisher Scientific). 41 μ l of the respective TMT reagent solution were transferred to the peptide sample of the respective DMSO control (V1-10). Directly after addition, samples were briefly vortexed. For the other samples (compound treated) 100 μ l were transferred to the respective remaining TMT reagent. Directly after addition, samples are briefly vortexed. Samples were incubated for 2 h at room temperature. Afterwards, 8 μ l of 5 % hydroxylamine were added and samples were incubated for 15 min to quench the reaction. After that, 120 μ l of each labeled aliquot incubated with **16** were combined into one sample and 120 μ l of each labeled aliquots incubated with DMSO were combined to a second one. Solvent was evaporated in a Speedvac device at 30°C until a dry white pellet was obtained.

Prior to nanoHPLC-MS/MS analysis, samples were fractionated into 10 fractions on a C18 column using high pH conditions to reduce the complexity of the samples, and thereby increasing the number of quantified proteins. Separation was performed at a flow rate of 50 μ l/min using 20 mM NH_4COO pH 11 in water as solvent A and 40 % 20 mM NH_4COO pH 11 in water premixed with 60 % acetonitrile as solvent B. Separation conditions were 95 % solvent A / 5 % solvent B isocratic for the first 10 min, to desalt the samples, followed by a linear gradient up to 25 % in 5 min, a second linear gradient up to 65 % solvent B in 60 min (75 min separation time in total) and a third linear gradient up to 100 % solvent B in 10 min. Afterwards, the column was washed at 100 % solvent B for 15 min and re-equilibrated to starting conditions. Detection was carried out at a valve length of 214 nm. The eluate between 15 and 100 min was collected in a meandering way over 10 collecting vials, changing vial position every 30 seconds. Each fraction was dried in a SpeedVac at 30°C until complete dryness and subsequently subjected to nanoHPLC-MS/MS analysis.

For nanoHPLC-MS/MS analysis, desalting was performed for 5 min with eluent flow to waste followed by back-flushing of the sample during the whole analysis from the pre-column to the PepMap100 RSLC C18 nano-HPLC column (2 μ m, 100 Å, 75 μ m ID \times 50 cm, nanoViper, Dionex, Germany) using a linear gradient starting with 95 % solvent A (water containing 0.1 % formic acid) / 5 % solvent B (acetonitrile containing 0.1 % formic acid) and increasing to 60 % solvent A 0.1 % formic acid / 40 % solvent B after 125 min using a flow rate of 300 nL / min.

The nano-HPLC was online coupled to the Quadrupole-Orbitrap Mass Spectrometer using a standard coated SilicaTip (ID 20 μ m, Tip-ID 10 μ m, New Objective, Woburn, MA, USA). Mass range of m/z 300 to 1650 was acquired with a resolution of 70000 for full scan, followed by up to ten high energy collision dissociation (HCD) MS / MS scans of the most intense at least doubly charged ions using a resolution of 35000 and a NCE energy of 35 %.

Data evaluation was performed using MaxQuant software (v.1.5.3.30)(Cox and Mann, 2008) including the Andromeda search algorithm and searching the human reference proteome of the Uniprot database. The search was performed for full enzymatic trypsin cleavages allowing two miscleavages. For protein modifications, carbamidomethylation was chosen as fixed and methionine oxidation and acetylation of the N-terminus were chosen as variable modifications. For relative quantification, the type “reporter ion MS2” was chosen. For lysine residues and peptide N-termini 10plex TMT labels were defined. The mass accuracy for full mass spectra was set to 20 ppm (first search) and 4.5 ppm (second search). The mass accuracy for MS/MS spectra was set to 20 ppm. False discovery rates for peptide and protein identification were set to 1 %. Only proteins for which at least two peptides were quantified were chosen for further validation. Relative quantification of proteins was carried out using the reporter ion MS2 algorithm implemented in MaxQuant. All experiments were performed in biological triplicates.

Melting Curves Calculation

To determine the melting point shifts between **16** and DMSO treated samples of each protein, an in-house developed Excel-Macro was used. Briefly, denaturation changes at different temperatures were tracked by the reporter ion intensity and observed in relation to the lowest temperature. The lowest temperature was set to value 1.

The relative fold changes were calculated as a function of temperature. The measuring points, which showed a sigmoidal trend, were fitted with the following equation using an iterative working macro for Microsoft Excel.

$$y = \text{bottom plateau} + \frac{(\text{top plateau} - \text{bottom plateau})}{1 + e^{-\left(\frac{a}{\text{Temp}}\right)^{-b}}$$

Where Top plateau is set to one, Temp is temperature, bottom plateau is a protein specific constant that defines the maximal denaturation and a and b are constants which describe the curve progression.

The melting point of a protein is defined as the temperature at which half of the protein has been denatured. This point aligns with the inflection point of the curve. The inflection point shows the highest slope of the curve, which is defined as the value of the first derivation. For hit identification, the requirements previously defined were followed.

In-lysate Stabilization Assay

The lysate of Jurkat cells was diluted to 2 g/L with PBS, treated either with **16** or with DMSO and incubated for 15 min at room temperature. A thermal treatment was performed in a PCR-Cycler to obtain a proper and equal temperature transfer to the samples. After temperature treatment, samples were cooled down to 4 °C and centrifuged for 25 min at 100.000 x g. The supernatant was mixed with Laemmli buffer and 40 μ L of the mixture were loaded on a gel to perform a SDS-PAGE. Afterwards, the proteins were transferred to a PVDF membrane. The membrane was blocked with 5 % BSA in PBS-T for 1 h and the first antibody (anti-PDE δ , #P5-22008, Thermo Scientific or anti-Na/K-ATPase: ab353, abcam) was incubated with the membrane at 4 °C overnight. The membrane was washed 3 times with PBS-T before the secondary antibody conjugated to HRP (anti-mouse, anti-rabbit) was incubated with the

membrane for 1 h. After washing the membrane three times, it was imaged by enhanced chemiluminescence (SuperSignal™ West Ferto Maximum Sensitivity Substrate).

Chemical Stability Assay

A 50 μM DMSO stock solution of compound **15** was diluted to a final concentration of 2 μM in aqueous buffer at pH 1.0 (in 0.1 M HCl), pH 7.4 (in PBS) or pH 9.0 (in NH_4COOH). Chemical stability of the compound was followed over 24h at four given time points: 0, 1h, 7h and 24h. All time points were measured simultaneously by LC-MS and the chemical stability was calculated relative to the zero time point.

Reaction of Compound 15 with Different Amino Acid Side-Chains

Compound **15** and the corresponding protected amino acid were mixed in PBS buffer at 5, 10, 20 and 30 μM concentrations. Adduct formation was followed after 30 and 60 minutes by HPLC using a Corona-charged aerosol detector.

Determination of K_D Values

Binding to PDE6 δ was validated and quantified by means of a displacement assay employing a fluorescent-tagged analog of the HMG-CoA reductase inhibitor Atorvastatin (Lipitor®), which also binds to PDE6 δ . K_D values were measured by fluorescence polarization. (Zimmermann et al., 2013) For direct titrations, increasing amounts of PDE6 δ were added to a solution containing 50–100 nM labelled small molecule in 200 μl PBS buffer. For displacement titrations, increasing amounts of the small molecules in DMSO were directly added to fluorescein-labelled atorvastatin (24 nM) and His₆-tagged PDE6 δ (40 nM) in 200 μl PBS-buffer (containing 0.05% CHAPS, 1% DMSO), keeping the concentration of fluorescein-labelled atorvastatin, PDE6 δ and DMSO constant.

General Information for Chemical Synthesis

All reactions involving air- or moisture-sensitive reagents or intermediates were carried out in flame dried glassware under an argon atmosphere. Dry solvents (THF, toluene, MeOH, DMF) were used as commercially available; CH_2Cl_2 was purified by the Solvent Purification System M-BRAUN Glovebox Technology SPS-800. Analytical thin-layer chromatography (TLC) was performed on Merck silica gel aluminium plates with F-254 indicator. Compounds were visualized by irradiation with UV light or potassium permanganate staining. Column chromatography was performed using silica gel Merck 60 (particle size 0.040–0.063 mm). ¹H-NMR and ¹³C-NMR were recorded on a Bruker DRX400 (400 MHz), Bruker DRX500 (500 MHz), INOVA500 (500 MHz) and DRX600 (600 MHz) at 300 K using CDCl_3 , CD_2Cl_2 , CD_3OD or $(\text{CD}_3)_2\text{SO}$ as solvents. All resonances are reported relative to TMS. Spectra were calibrated relative to solvent's residual proton and carbon chemical shift: CDCl_3 ($\delta = 7.26$ ppm for ¹H NMR and $\delta = 77.16$ ppm for ¹³C NMR); CD_2Cl_2 ($\delta = 5.32$ ppm for ¹H NMR and $\delta = 53.84$ ppm for ¹³C NMR); CD_3OD ($\delta = 3.31$ ppm for ¹H NMR and $\delta = 49.00$ ppm for ¹³C NMR); $(\text{CD}_3)_2\text{SO}$: $\delta = 2.50$ ppm for ¹H NMR and $\delta = 39.52$ ppm for ¹³C NMR). Multiplicities are indicated as: br s (broadened singlet), s (singlet), d (doublet), t (triplet), q (quartet), quin (quintet), m (multiplet); and coupling constants (J) are given in Hertz (Hz). High resolution mass spectra were recorded on a LTQ Orbitrap mass spectrometer coupled to an Acceka HPLC-System (HPLC column: Hypersyl GOLD, 50 mm x 1 mm, particle size 1.9 μm , ionization method: electron spray ionization). Atorvastatin was purchased from Sequoia Research Products. All other chemicals and solvents were purchased from Sigma-Aldrich, Fluka, TCI, Acros Organics, ABCR and Alfa Aesar. Unless otherwise noted, all commercially available compounds were used as received without further purifications. Details of chemical synthesis and the relevant NMR spectra are included in [Methods S1](#).

QUANTIFICATION AND STATISTICAL ANALYSIS

All data fitting and statistical analysis were performed using GraphPad Prism version 5.03 for Windows, GraphPad Software, La Jolla, California USA, www.graphpad.com. Statistical values including the exact n and statistical significance are also reported in the Figure Legends. Intensities of the PDE6 δ immunoblot bands (Image Lab) are plotted as mean \pm CI of 95% (n = 4). Statistical significance was defined as $p \leq 0.05$ and determined by one-way ANOVA with Bonferroni's post-tests.

DATA AND SOFTWARE AVAILABILITY

Data Resources

The atomic coordinates and structure factors for the crystal structure of inhibitor **15** covalently bound to PDE6 δ have been deposited in the PDB (<http://www.pdb.org>) under the accession code PDB: 5NAL.